

# SHOCK WAVE CAPTURING WITH MULTI-GRID ACCELERATED, SOLUTION ADAPTIVE, CARTESIAN GRID BASED NAVIER STOKES SOLVER

**Emre KARA\***

University of Gaziantep  
Mechanical Engineering Dept.  
Gaziantep, TURKEY  
emrekara@gantep.edu.tr

**Ahmet İhsan KUTLAR**

University of Gaziantep  
Mechanical Engineering Dept.  
Gaziantep, TURKEY  
aikutlar@gantep.edu.tr

**Mehmet Halûk AKSEL**

Middle East Technical University  
Mechanical Engineering Dept.  
Ankara, TURKEY  
aksel@metu.edu.tr

*Received: 16<sup>th</sup> June 2016, Accepted: 17<sup>th</sup> August 2016*

## ABSTRACT

*Cartesian grids employ specially designed algorithms to generate automatic grids for complex geometries and to simulate flows around such geometries regardless of the body shape and number of bodies. The main advantage of Cartesian methods over the body-conformal approach is that without regard to drawbacks of the geometric complexity of the embedded boundaries, the computational grid does not alter except close to all boundaries where cutcells are employed. In this study, implementation of generated two-dimensional adaptive refinement/coarsening scheme codes is appended to the developed compressible flow solver by using special Cartesian-based algorithms. Cartesian grids are generated by constructing a quadtree based data structure in two-dimensional flows. By means of solution adaptation, a finer grid is obtained around a shock wave. Convergence rate is increased with multi-grid method. Thus, a “hands-off”, Cartesian grid generator based flow solver is implemented in object-oriented FORTRAN programming language.*

*The solutions are validated by comparing the results with experimental and numerical data available in literature for the supersonic flow around NACA 0012 airfoil. Employing the solution adaptation techniques, Mach contours of the flow around the wing have verified and captured the shock wave by the developed GeULER-NS (cartesian-Grid-generator-with-eULER-and-Navier-Stokes-flow-solver) code.*

**Keywords:** *Cartesian Grid Generation, Object-oriented Programming, Solution Adaptation, Multi-grid Method.*

## ÇOK KATMANLI AĞLA HIZLANDIRILMIŞ, ÇÖZÜM UYARLAMALI, KARTEZYEN AĞ TEMELLİ NAVIER-STOKES ÇÖZÜCÜSÜ İLE ŞOK DALGASI YAKALANMASI

## ÖZ

*Kartezyen ağlar, karmaşık geometriler için otomatik ağ oluşturma ve bu gibi geometriler etrafında akışın gövde şeklinden ve sayısından bağımsız şekilde benzetim kurmak için özellikle tasarlanmış algoritmalar kullanırlar. Geleneksel gövde-uyumlu yaklaşıma göre Kartezyen yöntemlerinin belirgin üstünlüğü gömülü sınırların geometrik karmaşıklığından bağımsız olarak hesaplama ağının, kesik-hücrenin kullanıldığı sınırlar dışında, değişmemesidir. Bu çalışmada, geliştirilen sıkıştırılabilir akış çözücüsüne, kapalı yüzeyler çevresinde Kartezyen temelli algoritmalar kullanılarak iki-boyutlu uyarlanabilir geliştirme/genişleme şema kodları ilave edilmiştir. Kartezyen ağlar, Kartezyen hücrelerinin birbirlerine bağlanmalarını sağlamak için oluşturulan, iki-boyutlu akışlarda dörtlü ağaç temelli veri yapısı kullanarak üretilmiştir. Çözüm uyarlaması marifetiyle şok dalgaları çevresinde daha ince ağ örgüsü elde edilmiştir. Yakınsama oranı çok katmanlı ağ yöntemi ile artırılmıştır. Sonuçta, kullanıcı müdahalesine gerek olmayan, nesne tabanlı FORTRAN programlama dilinde Kartezyen ağ üreticisi temelli akış çözücüsü uygulanmıştır.*

*Literatürde mevcut olan NACA 0012 kanadı çevresindeki sesüstü akışlar için deneysel ve nümerik verilerle çözümler karşılaştırılarak doğrulanmıştır. Çözüm uyarlama yöntemlerini kullanarak, geliştirilen GeULER-NS kodu tarafından kanat çevresindeki Mach kontürleri şok dalgasını doğrulamış ve yakalamıştır.*

**Anahtar Kelimeler:** *Kartezyen Ağ Üretimi, Nesne Tabanlı Programlama, Çözüm Uyarlaması, Çok Katmanlı Ağ Yöntemi.*

\* Corresponding Author

## 1. INTRODUCTION

With the development of digital computers, Computational Fluid Dynamics (CFD) has become an obligatory and inevitable tool in the field of fluid dynamics; however, turbulence modelling, selection of the accurate numerical techniques, algorithmic efficiency, surface modelling and grid generation around complicated and multi-component geometries are still barriers to CFD development. Therefore, various new approaches to tackle with these problems are still being developed.

Cartesian methods are a special class of unstructured methods (see Figure 1). In the last decade, there has been a renewal of vigour towards the application of adaptive Cartesian grid generation algorithms especially to the problems involving complex geometries. In comparison with body-fitted grid generation schemes, adaptation of inherently non-body-fitted Cartesian grid generation techniques to complex geometries is very easy to implement. Structured grids have the advantage of having simple data structures, but they are usually limited to simple, single-body geometries and are not suitable for multi-branched shapes. Cartesian grids, however, being a special class of unstructured ones, have beneficiary effects in the solution of partial differential equations resulting from their characteristic form of discretized finite-volume representation, for example, in the solution of Navier-Stokes equations involving irregular and multi-element boundaries. With regard to traditionally used unstructured grid methods, the Cartesian grid methods use exclusive line iteration technology and multi-grid techniques on complex geometries. The procedure is also very quick in comparison with the other unstructured grid generation techniques.

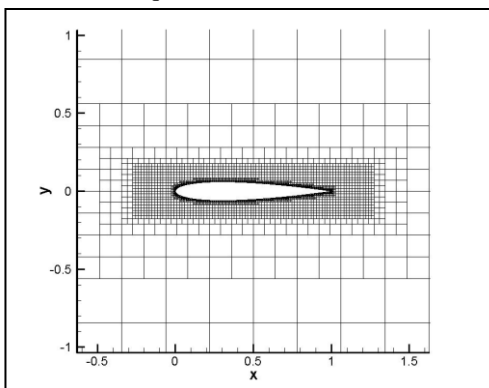


**Figure 1.** Cartesian grid around a NACA0012 airfoil

The main advantage of Cartesian methods over the body-conformal approach is that without regard to drawbacks of the geometric complexity of the embedded boundaries, the computational grid does not alter except close to all boundaries where cutcells are employed. Another important advantage of Cartesian methods is that any kind of adaptation is very easy to

implement. By means of solution adaptation, for instance, a finer grid can be obtained around a shock wave. Hence, very high accuracy levels can be obtained without increasing cell number and computational time significantly. The governing equations are discretized on a Cartesian grid, which does not conform to the immersed boundaries. This greatly simplifies grid generation and also retains the relative simplicity of the governing equations in Cartesian coordinates. In addition, this method also has a significant advantage over the conventional body-fitted approach in simulating flows with moving boundaries, complicated shapes, or topological changes [1].

The present study focuses on the generation of locally refined hierarchical Cartesian grids applicable to Euler and Navier-Stokes equations involving two-dimensional irregular geometries providing solutions relatively easy to realize and accurate for the case of compressible flows. The computational procedures regarding two-dimensional domains are handled in detail using specially designed Cartesian grid algorithms.

The main objective of this study is to develop an automatic, adaptive Cartesian grid based compressible flow solver that is capable of solving viscous flows in two-dimensional geometries. The solver uses finite-volume type discretization with an explicit time marching scheme. Local time stepping and multi-grid methods are employed to accelerate convergence. A quadtree Cartesian grid generator is constructed using special Cartesian algorithms and object-oriented programming of FORTRAN. A Cartesian grid based, finite volume solver is developed to produce accurate solutions of inviscid flows over two-dimensional airfoils. Viscous terms of Navier-Stokes equations are implemented into the flow solver. As the result, a “hands-off” flow solver is implemented in object-oriented FORTRAN programming language. The code is validated by comparing with experimental results and verified by numerical results. In the previous studies of authors, examples of the Cartesian grid are presented which were obtained by using quadtree approach [2], the efficiency of quadtree data structure is tested with respect to other data structure techniques in two dimensions [3] and locally refined hierarchical Cartesian grids for two-dimensional irregular geometries are solved in GeULER (Cartesian Grid generator with **eULER** flow solver) for the case of inviscid compressible flows around single airfoils [4] and multi-element airfoils [5]. Also, an octree-based solution-adaptive Cartesian grid generator and Euler solver for the simulation of three-dimensional inviscid compressible flows is generated by GeULER3D (Cartesian Grid generator with **eULER** flow solver for **three-dimensional** applications) [6]. The extension of the flow solver GeULER to GeULER3D can be summarized as follows:

•The process of grid generation is arguably straightforward in two dimensions but requires a series of computational operations in a three-dimensional problem around a solid geometry for an efficient execution. Watertight, closed surface triangulation of the solid geometry is required.

•Data structure has one dimension more (i.e. octree).

•Curvature adaptation is not allowed; instead cut-cell adaptation is supported by ghost-cell method.

•Governing flow solver equations are the same but the third dimension is added for GeULER3D.

•Other details can be found by comparing this article with the authors' previously published article [6].

## 2. MATERIALS AND METHODS

In this section, the integral forms of two-dimensional Navier-Stokes equations are presented. Considering an arbitrary control cell the conservative integral form of Navier-Stokes equations is generated using Gauss divergence theorem as follows:

$$\frac{\partial}{\partial t} \int_A \mathbf{Q} dA + \int_S (\mathbf{F} \cdot \mathbf{n}) dS = \int_S (\mathbf{G} \cdot \mathbf{n}) dS \quad (1)$$

where  $A$  is the cell area,  $S$  is the perimeter of the contour surrounding  $A$ ,  $\mathbf{F}$  and  $\mathbf{G}$  are the inviscid and viscous flux vectors, respectively.  $\mathbf{Q}$  represents the vector of any conserved variable such as density,  $\rho$ ,  $x$  and  $y$ -velocity components,  $u$  and  $v$  respectively.

Flow variables computed from Navier-Stokes equations are stored at the centroids of each cell assuming that the variables of each cell do not vary throughout the cell. Semi-discrete form of Eq. (1) can be written as the sum of the fluxes through each cell as follows:

$$A \frac{\partial \mathbf{Q}}{\partial t} + \sum_{i=1}^4 (\mathbf{F} \cdot \mathbf{n}) \Delta S = \sum_{i=1}^4 (\mathbf{G} \cdot \mathbf{n}) \Delta S \quad (2)$$

It is assumed that convective fluxes are constant on surfaces and time stepping of the conserved variables on faces is inherited from the one calculated on centroid of the area. The residuals,  $Res$ , of each cell can be defined in the following equation:

$$\frac{\partial \mathbf{Q}}{\partial t} = -\frac{1}{A} Res(\mathbf{Q}) \quad (3)$$

Following spatial discretization, the time derivatives of the conserved variables are now discretized to obtain almost-zero residuals by iteration and CFL cut-back procedure is achieved. Details can be found in [5].

During execution of the flow solver, Cartesian grid based structure makes it easier to locally refine or coarsen grids on the critical regions such as shock-based discontinuities, stagnation points, shear layers, etc. This phenomenon is called as solution adaptation which increases the accuracy of the results. In this study, the solution adaptation technique is based primarily on the work of Marshall [7]. Three characteristic lengths,  $\zeta$ , of the control volume are used to gain possession of changing conservative variables from one cell to its neighbouring cells by:

$$\zeta_{D,x} = |\nabla \cdot \mathbf{u}| V^{0.5}; \zeta_{D,y} = |\nabla \cdot \mathbf{v}| V^{0.5}; \zeta_{D,z} = |\nabla \cdot \mathbf{w}| V^{0.5} \quad (4.a)$$

$$\zeta_{C,x} = |\nabla \times \mathbf{u}| V^{0.5}; \zeta_{C,y} = |\nabla \times \mathbf{v}| V^{0.5}; \zeta_{C,z} = |\nabla \times \mathbf{w}| V^{0.5} \quad (4.b)$$

where subscripts  $D$  and  $C$  stand for divergence and curl of the velocity vectors, respectively. Reference values, the standard deviation of these three characteristic lengths, are calculated for entire solution domain by:

$$\sigma_D = \frac{1}{N} \sum_{i=1}^N \zeta_{D,x}^2 + \zeta_{D,y}^2 + \zeta_{D,z}^2; \quad \sigma_C = \frac{1}{N} \sum_{i=1}^N \zeta_{C,x}^2 + \zeta_{C,y}^2 + \zeta_{C,z}^2 \quad (5)$$

where  $N$  is the total number of solution domain cells. Cells are flagged for refinement or coarsening using the threshold values  $t_r$  and  $t_c$  for refinement and coarsening respectively, following the criteria below:

$$\text{if } (\zeta_{D,x} + \zeta_{D,y} + \zeta_{D,z} > t_r \sigma_D) \ \& \ (\zeta_{C,x} + \zeta_{C,y} + \zeta_{C,z} > t_r \sigma_C) \ \text{refine} \quad (6.a)$$

$$\text{if } (\zeta_{D,x} + \zeta_{D,y} + \zeta_{D,z} < t_c \sigma_D) \ \& \ (\zeta_{C,x} + \zeta_{C,y} + \zeta_{C,z} < t_c \sigma_C) \ \text{coarsen} \quad (6.b)$$

where  $t_r$  is taken as 1 and  $t_c$  is taken as 0.1. An example of solution adaptation is shown in Figure 2.

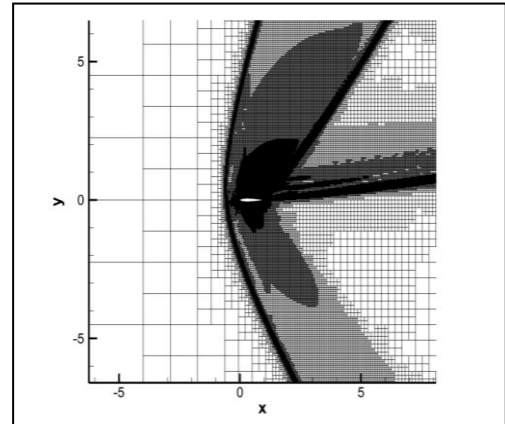


**Figure 2.** Representation of solution adaptation around NACA0012 airfoil.

In the current study, two different spatial discretization techniques are used for viscous flows. First one is a variant of Riemann Solver, namely Roe's Approximate Riemann Solver [8]; second one is a flux-vector splitting method; Liou's Advection Upstream Splitting Method [9]. Viscous flux calculations are carried out by averaged gradient from left cell's centroid and right cell's centroid of the corresponding face using Gauss' divergence theorem.

The viscous fluxes,  $\mathbf{G}$ , are averaged at the face cell centres between the cell centroid and its neighbour cell centroid. Cell centroid gradients are available from convective term calculation. The surface gradient is computed with the average gradient method in which once the gradients at each cell centroid are known, two cells sharing a face transfer their gradients' average to this face. This method loops for four faces of each cell.

After spatial and temporal discretization of the problem, the main issue of the solution is the convergence. Convergence of unstructured grids is generally slower than structured grids, since they require more complex data structures, more care in boundary layer treatment. In both grid types, residual of the discretized flux formulation decreases by iterative techniques. In unstructured grids, during these iterations, there happen two types of errors, namely, high-frequency and low frequency errors. The low-frequency errors occur on the near solid boundary fine grids that are slow to converge whereas the high-frequency errors occur on coarse grids that converge quickly. The multi-grid method has the mission of increasing time spent on coarse grids rather than fine grids and propagates high-frequency error disturbances more quickly. Therefore, less computational effort is consumed and as a result, the convergence rate can increase by several hundred times.

Multi-grid method's effect on convergence time for a transonic flow is shown in Figure 3. As one can see from this figure, multi-grid cycle (red lines) converges much faster than cycle with no multi-grid (green lines). Also, multi-grid method makes at least four times faster convergence with respect to solution with no multi-grid. The procedure iteratively solves the problem till logarithm of root-mean-square (rms) of the density residual drops below a predefined value. Red and green lines reach  $10^{-9}$  and  $10^{-7}$  as the rms values. Consequently, faster solution with multi-grid also gives better accuracy.

In this study, the Cartesian grid is obtained by using the quadtree approach to store the grid information with a direct and easy path for the cell-neighbor identification. The root cell, inherently without any parent, is the starting point of a quadtree data structure. The root cell is a square Cartesian cell and four equal face child cells are obtained by subdividing each cell. The grid typically begins with a single root cell, and grows by a recursive subdivision of each cell into its four child cells. Each child is geometrically contained within the boundaries of the root cell, and is located logically below the root cell in the tree. The hierarchical spatial subdivision defines simplified four-level quadtree classes beginning after the root cell as shown in Figure 4.

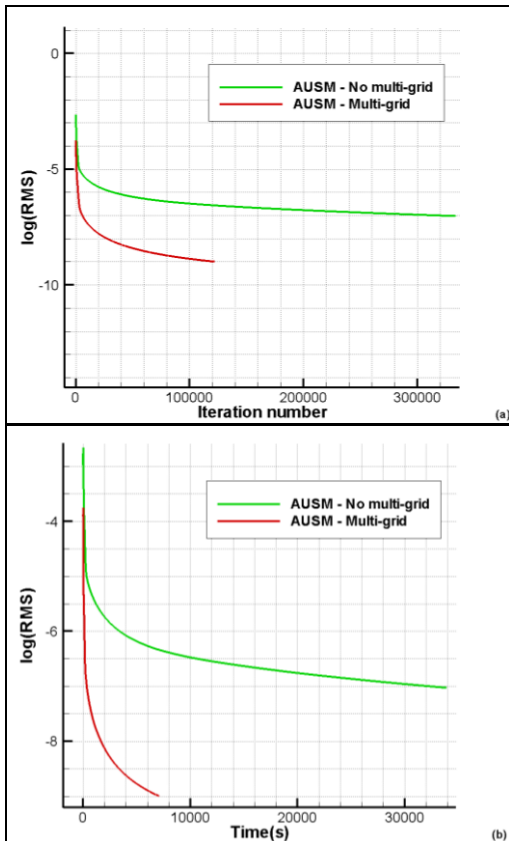


**Figure 3.** Transonic flow over NACA 0012: (a) Convergence histories and (b) residuals versus CPU time;  $M_\infty = 0.8$ ,  $\theta = 10.0^\circ$ ,  $Re = 1000$ .

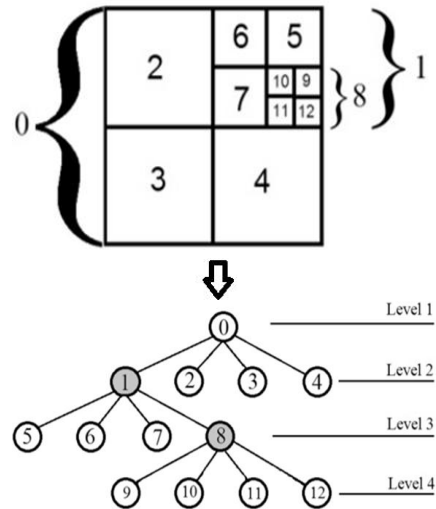


**Figure 4.** Quadtree data structure representation

Explicit Runge-Kutta multistage time stepping is employed for all solutions. Implicit time stepping techniques can be integrated into the current study for faster convergence and for comparing results with reliable results of explicit scheme, but implicit schemes are difficult to apply on unstructured grids; explicit schemes converge but slower than regular structured grids. As applied in this study, complicated data structure problem can be prevented by the use of Cartesian grids and multi-grid methods can increase convergence rate by 100 folds. Details can be found in the corresponding author's Ph.D. thesis [10].

Least squares reconstruction (minimum energy) method is used in the flow solver to calculate the primitive variable gradients in each cell volume.

The main program is named GeULER-NS (Cartesian Grid generator with eULER and Navier Stokes flow solver). When the program starts, it calls all the required information for the initialization from a text file, following that executes mesh generator and flow solver, and finally exports the output of flow simulation, based on information initially provided.

### 3. RESULTS

The case of viscous study is supersonic flow at  $M_\infty = 2.0$ , angle-of-attack of  $10.0^\circ$  &  $Re = 1000$  over NACA 0012 airfoil. The purposes of this test are to capture thin detached, bow shock wave and to compare the pressure distribution along the surface of airfoil with three different reference studies. To compare the results, the data taken from the studies of Arminjon and Madrane [11], De Palma et al. [12] and Liu et al.

[13] are used. First two references are selected because of their successful benchmark applications [14, 15] and Liu's study [13] is selected because their study used a new immersed boundary method called radial basis function immersed boundary method (RBFIBM) instead of body fitted solutions as in Arminjon and Madrane [11] and De Palma [12].

Properties for supersonic flow around NACA 0012 are tabulated in Table 1. In Figure 5.a, the convergence histories for all cases are given where the lowest iteration number of convergence occurs in AUSM with three solution refinement (SR). However, as seen in Figure 5.b, AUSM with three SR is second slowest case among all cases. The surface pressure distribution results of AUSM are favorably compared with three references mentioned in Figure 6. GeULER-NS with three refinement levels is not depicted here, because it coincides almost exactly with two SR levels. GeULER-NS results agreed well with all three references, especially with two SR level.

**Table 1.** Input file for supersonic flow around NACA 0012

<b>Cartesian Grid</b>				
Outer boundary size factor	18			
Number of successive divisions to generate uniform grid	4			
Boundary size factor for box-adaptation (in x&y directions)	1.5 & 2.5			
The size of the cells with respect to maximum body dimension	0.01			
Cut-cell adaptation cycle	2			
Curvature adaptation cycle	1			
Maximum level of cell	20			
<b>Boundary Conditions</b>				
Mach Number	2.0			
Angle of Attack ( $^\circ$ )	10.0			
Reynolds Number	1000			
Prandtl Number	0.72			
Specific heat ratio of the fluid	1.4			
Free stream temperature in Kelvin	273.15			
<b>Solution Parameters</b>				
Solution schemes for the flux	AUSM			
Multiplication criteria for refinement	0.05			
Numbers of refinement and coarsening cycle	0	1	2	3
<b>Convergence Parameters</b>				
Multi-grid Cycle Number	7			
Residual exponent for the limit of convergence	-8			
<b>Computational Details</b>				
Resolution (nodes)	40448	79588	120576	192116
Time Step (seconds)	0.25	0.25	0.25	0.25
CPU Time (seconds)	2147	2456	2600	3377

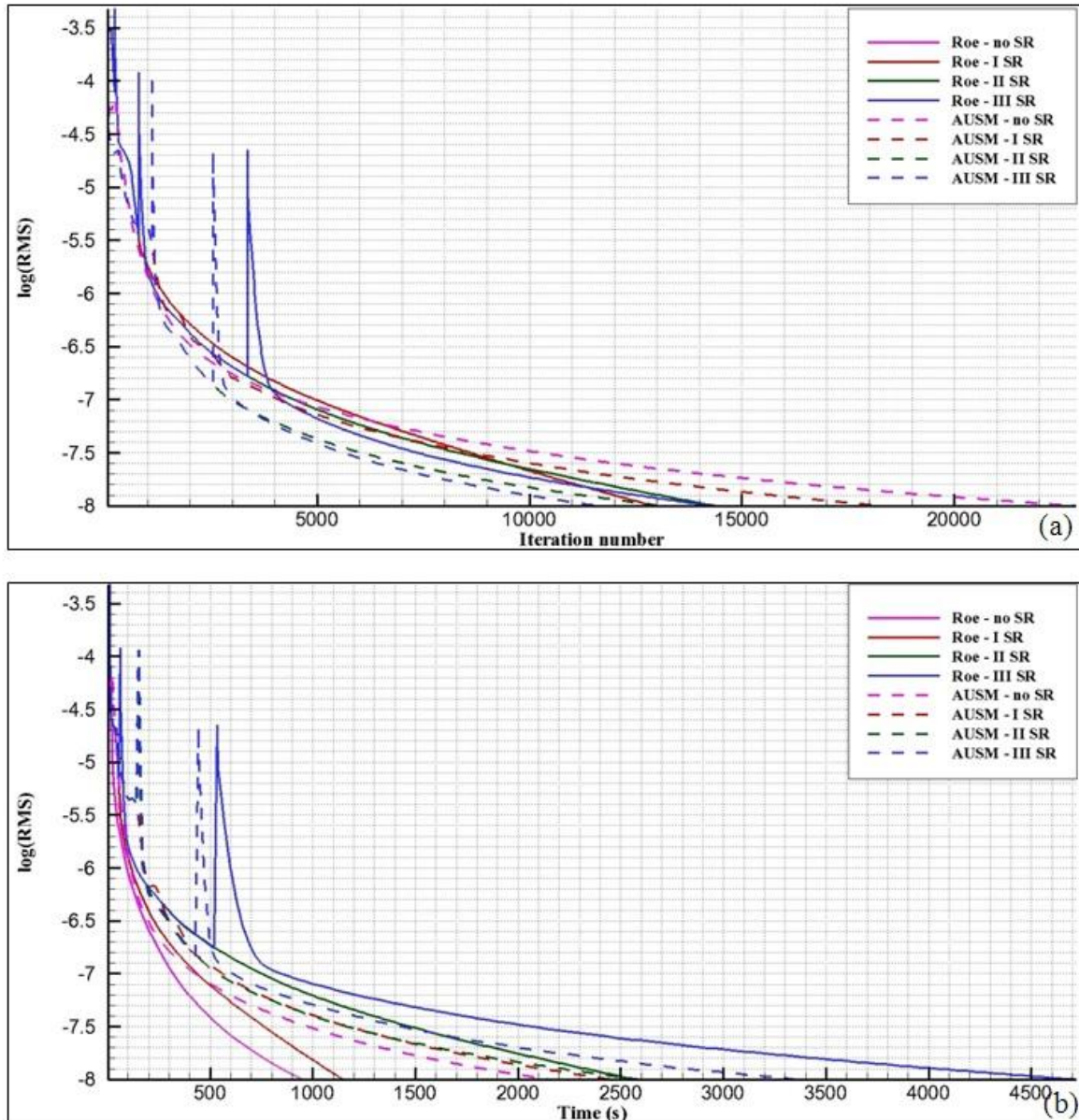


**Figure 5.** Supersonic test case of NACA 0012: (a) Convergence histories and (b) residuals versus CPU time;  $M_\infty = 2.0$ ,  $\theta = 10.0^\circ$ ,  $Re = 1000$ .

Figure 7 shows the Mach contours obtained by using different SR levels for both AUSM and Roe's flux construction method. The most successful representation is captured in Figure 7.c and compared with the reference studies in Figure 8. The figure shows that sharp bow shock is successfully captured and Mach contours are very similar to all three reference studies with clean resolution of boundary layer and also capturing of the trailing edge detachment of the boundary layer. In Figure 8.e., a close-up view of test case 8, i.e. AUSM with three SR, shows the detachment of boundary layer between 0.75-0.8 from the tip of airfoil.

In the studies of Arminjon and Madrane [11] and Liu et al. [12] lift coefficient is not given for this

supersonic flow case. The calculated lift coefficients by GeULER-NS and those given by De Palma et al. [12] with Euler implicit scheme are presented in Table 3 in comparison with the results given in Table 2. Case 8, GeULER-NS result with three SR (AUSM), slightly overestimates by 0.4 % in comparison with Cambier [14]. The case overestimates the result of Müller et al. [15] by 1.6 %, gives more accurate result than De Palma et al. [12] with respect to Cambier's benchmark study. Lift coefficient result of Müller et al. [15] is slightly overpredicted by GeULER-NS than De Palma's prediction in absolute value. Four SR solution of Roe and AUSM schemes does not change the lift coefficient results that they are almost exactly the same with three SR levels. So, they are not mentioned in this study.

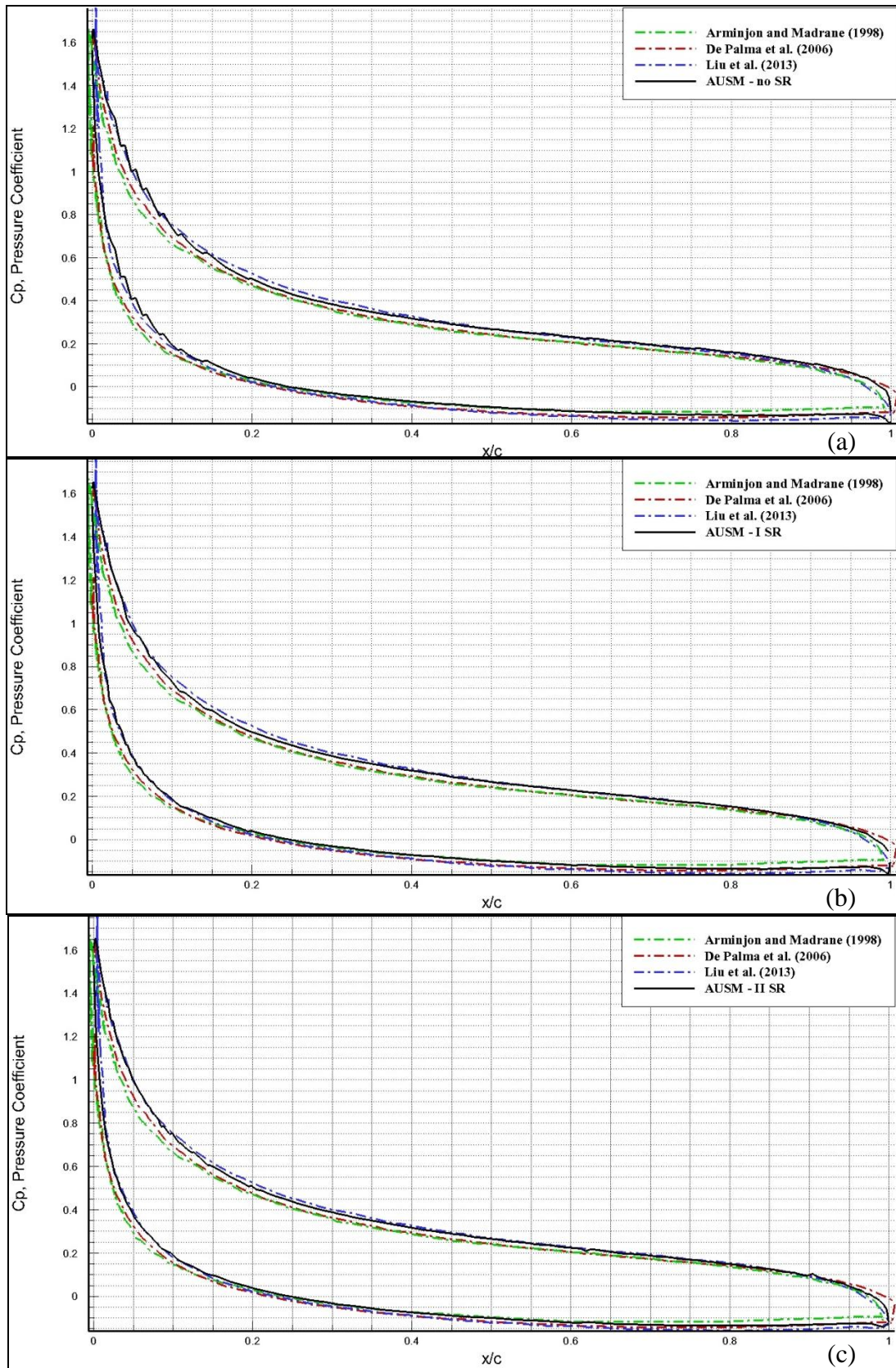


**Figure 6.** Pressure coefficient distribution results of De Palma et al. [12], Liu et al. [13] and Arminjon and Madrane [11] in comparison with GeULER-NS results along the surface of NACA 0012 airfoil with (a) no SR (b) one SR, (c) two SR;  $M_\infty = 2.0$ ,  $\theta = 10.0^\circ$ ,  $Re = 1000$ .

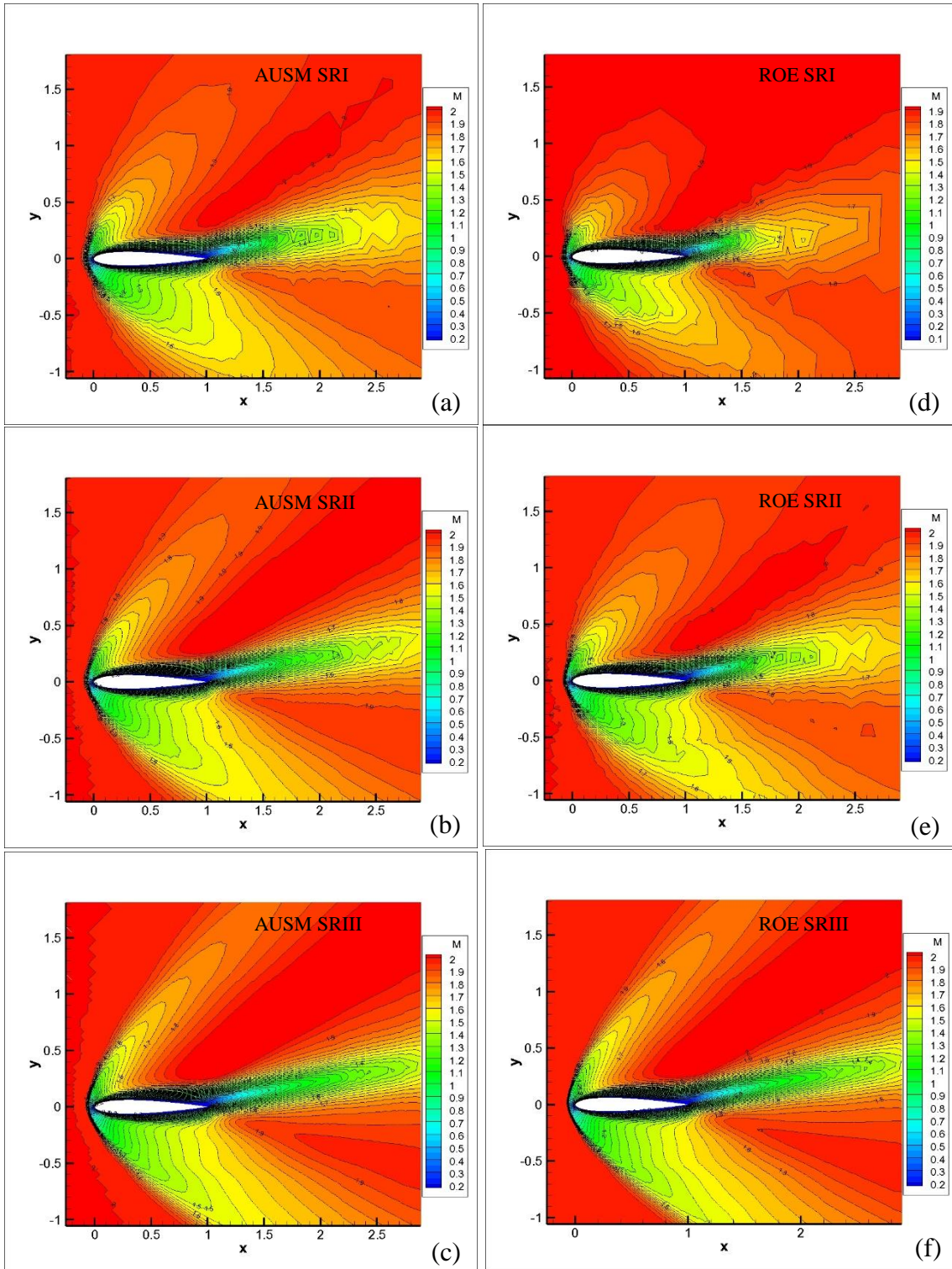


**Figure 7.** GeULER-NS results of Mach number contours around NACA 0012 airfoil by using AUSM with (a) one SR (b) two SR, (c) three SR; by using Roe’s approximate Riemann solver with (d) one SR, (e) two SR, (f) three SR;  $M_\infty = 2.0$ ,  $\theta = 10.0^\circ$ ,  $Re = 1000$ .

**Table 2.** Lift coefficient results of reference benchmark studies for supersonic viscous flow around NACA 0012

Study	Lift Coefficient, $c_l$
Cambier [14]	0.3427
Müller et al. [15]	0.3388



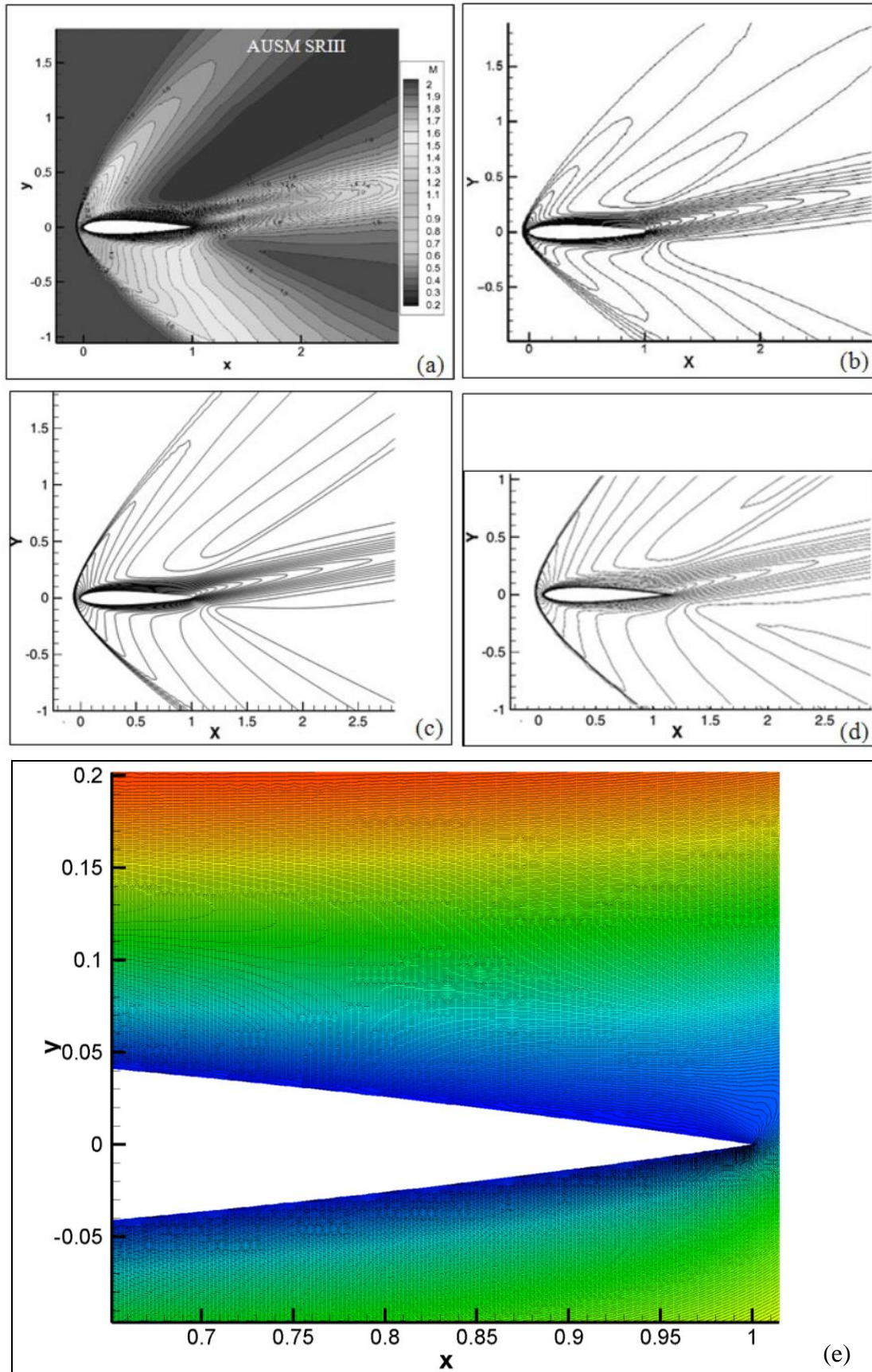


**Figure 8.** Mach number contours around NACA 0012 airfoil (a) by using AUSM with three SR (GeULER-NS result); in comparison with Mach number contours of (b) De Palma et al. [12], (c) Liu et al. [13] and (d) Arminjon and Madrane [11]; (e) a close-up view (AUSM with three SR) ;  $M_\infty = 2.0$ ,  $\theta = 10.0^\circ$ ,  $Re = 1000$ .

**Table 3.** Lift coefficient results of GeULER-NS for supersonic viscous flow around NACA 0012 airfoil

Case no	Scheme	Ref. no	Lift Coefficient, $C_l$	% error with respect to Cambier [14]	% error with respect to Müller et al. [15]
1 (Roe – No SR)	Roe	0	0.3484	1.7	2.8
2 (Roe – 1 SR)	Roe	1	0.3480	1.5	2.7
3 (Roe – 2 SR)	Roe	2	0.3505	2.3	3.5
4 (Roe – 3 SR)	Roe	3	0.3505	2.3	3.5
5 (AUSM – No SR)	AUSM	0	0.3667	7.0	8.2
6 (AUSM – 1 SR)	AUSM	1	0.3641	6.2	7.5
7 (AUSM – 2 SR)	AUSM	2	0.3510	2.4	3.6
8 (AUSM – 3 SR)	AUSM	3	0.3442	0.4	1.6
De Palma et al. [12]	Euler	coarse	0.3296	-3.8	-2.7
De Palma et al. [12]	Euler	medium	0.3335	-2.7	-1.6
De Palma et al. [12]	Euler	fine	0.3353	-2.2	-1.0

#### 4. CONCLUSION

In current study, an original GeULER-NS grid generator and flow solver program using object-oriented FORTRAN programming language is designed, coded and executed. Implementation of generated adaptive refinement/coarsening scheme codes are appended to the developed compressible flow solver by using special Cartesian-based algorithms, namely Ray-Casting method, cutcell adaptation and curvature adaptation around closed bodies.

Validation of the numerical results is accomplished by comparison with the experimentally obtained data from the flow around NACA 0012 airfoil. A supersonic flow at free stream Mach number of 2.0 around NACA0012 airfoil is tested to predict pressure distributions around it and Mach contours of the flow are depicted by using the developed GeULER-NS code with one, two and three SR levels. Three SR's of AUSM scheme give the best pressure distribution results and smoothest depiction with respect to experimental data and Liu's [13] numerical study. Sharp bow shock is successfully captured and Mach contours are very similar to all selected reference studies with clean resolution of boundary layer and also capturing of the trailing edge detachment of the boundary layer. Additionally, lift coefficient results of GeULER-NS are also compared with experimental studies. GeULER-NS result with three SR (AUSM), slightly overestimates by 0.4 % in comparison with Cambier [14]. The case overestimates the result of Müller et al. [15] by 1.6 %, gives more accurate result than De Palma et al. [12] with respect to Cambier's benchmark study. Result of Müller et al. [15] is slightly overpredicted by GeULER-NS than De Palma's prediction in absolute value.

As a final comment on this supersonic flow test case, resemblances and successful depictions between three references and current study in pressure coefficient distributions, Mach contours and lift coefficient results are very encouraging for GeULER-NS flow solver. The solver algorithms can be extended for three-dimensional laminar flows before moving into the turbulent flow simulation cases. All results reveal the effectiveness of the program and suffice in accuracy and convergence.

#### 5. REFERENCES

- [1] Ye, T., Mittal, R., Udaykumar, H. S., & Shyy, W. "An accurate Cartesian grid method for viscous incompressible flows with complex immersed boundaries", *Journal of Computational Physics*, No: 156(2), pp. 209–240, 1999. [DOI:[10.1006/jcph.1999.6356](https://doi.org/10.1006/jcph.1999.6356)]
- [2] Kara, E., Kutlar, A.I., Aksel M.H., "Quad-Tree Based Geometric-Adapted Cartesian Grid Generation", *8th International Conference on Continuum Mechanics (CM '13)*, 16–19 July, Series No. 14, Rhodes Island/Greece, 2013. [<http://www.wseas.us/e-library/conferences/2013/Rhodes/HYDRECO/HYDR-ECO-01.pdf>]
- [3] Kara, E., Kutlar, A.I., Aksel M.H., "A Quad-Tree Based Automatic Adaptive Cartesian Grid Generator with Applications on Multi-Element Airfoils", *7th Ankara International Aerospace Conference (AIAC'13)*, 11-13 September, Ankara/Turkey, 2013. [<http://aiac.ae.metu.edu.tr/db/serv.php?Paper=AIAC-2013-027>]
- [4] Kara, E., Kutlar, A.I., Aksel M.H., "A solution adaptive multi-grid Euler solver on two-dimensional Cartesian grids", *8th Ankara International Aerospace*

Conference (AIAC'15), 10–12 September, Ankara/Turkey, 2015. [<http://aiac.ae.metu.edu.tr/db/serv.php?Paper=AIAC-2015-133>]

[5] Kara, E., Kutlar, A.I., Aksel M.H., “A Solution Adaptive Cartesian Grid Based Euler Solution for Compressible Flow around BOEING TR-1322 Multi-element Airfoil”, *Nevsehir Science and Technology Journal*, Vol.4, No:1, 69–80, 2015. [DOI: [10.17100/nevbiltek.66399](https://doi.org/10.17100/nevbiltek.66399)]

[6] Kara, E., Kutlar, A.I., Aksel, M.H., “An octree-based solution-adaptive Cartesian grid generator and Euler solver for the simulation of three-dimensional inviscid compressible flows”, *Progress in Computational Fluid Dynamics*, Vol.16, No: 3, pp.131–145, 2016. [DOI: [10.1504/PCFD.2016.076247](https://doi.org/10.1504/PCFD.2016.076247)]

[7] Marshall, D. “Fully automated Cartesian grid CFD application for MDO in high speed flows”, *NASA Technical Report*, pp 1-254, 2003.

[8] E.F. Toro, “Riemann Solvers and Numerical Methods for Fluid Dynamics”, 3rd Edition, Springer-Verlag Publishing, Berlin, 2009.

[9] Liou, M.S., Steffen, C.J., “A New Flux Splitting Scheme”, *Journal of Computational Physics*, Vol.107, No: 1, pp. 23–39, 1993. [DOI:[10.1006/jcph.1993.1122](https://doi.org/10.1006/jcph.1993.1122)]

[10] E. Kara, “Development of a Navier Stokes Solver for Compressible Flows on Cartesian Grids with Aerodynamics Applications”, Doctoral dissertation, University of Gaziantep, Gaziantep, Turkey, 2015.

[11] Arminjon, P., Madrane, A., “A Staggered Lax-Friedrichs Type Mixed Finite Volume/Finite Element Method for the Simulation of Viscous Compressible Flows on Unstructured Triangular Grids”, *AIAA Journal*, pp. 1–27, 1998. [<http://www.crm.umontreal.ca/pub/Rapports/2500-2599/2575.pdf>]

[12] De Palma, P., De Tullio, M.D., Pascazio, G., Napolitano, M., “An Immersed-Boundary Method for Compressible Viscous Flows”, *Computers & Fluids*, Vol: 35, No: 7, pp. 693–702, 2006. [DOI: [10.1016/j.compfluid.2006.01.004](https://doi.org/10.1016/j.compfluid.2006.01.004)]

[13] Liu, J., Zhao, N., Hu, O., Goman, M., Li, X. K., “A New Immersed Boundary Method for Compressible Navier–Stokes Equations”, *International Journal of Computational Fluid Dynamics*, Vol: 27, No: 3, pp. 151–163, 2013. [DOI: [10.1080/10618562.2013.791391](https://doi.org/10.1080/10618562.2013.791391)]

[14] L. Cambier, “Computation of Viscous Transonic Flows Using an Unsteady Type Method and

a Zonal Grid Refinement Technique”, *Numerical Simulation of Compressible Navier-Stokes Flows*, pp. 105–122, Vieweg Teubner Verlag Publishing, Germany, 1987. [DOI: [10.1007/978-3-322-87873-1\\_6](https://doi.org/10.1007/978-3-322-87873-1_6)]

[15] B. Müller, T. Berglind, A. Rizzi, “Implicit Central Difference Simulation of Compressible Navier-Stokes Flow Over a NACA0012 Airfoil”, *Numerical Simulation of Compressible Navier-Stokes Flows*, pp. 183–200, Vieweg Teubner Verlag Publishing, Germany, 1987. [DOI: [10.1007/978-3-322-87873-1\\_11](https://doi.org/10.1007/978-3-322-87873-1_11)]

## VITAE

### Dr. Emre KARA

Emre Kara has received his B.S. degree in Mechanical Engineering from Middle East Technical University, Ankara, Turkey. He joined University of Gaziantep on September 12, 2006 as a Research Assistant in Mechanical Engineering Department. He holds a Ph.D. degree from the same university and department, with specializations in computational fluid dynamics and biomechanical engineering, mesh generation methods, object-oriented programming, aerodynamics and algorithms for scientific computing.

### Assoc. Prof. Dr. Ahmet İhsan KUTLAR

A. İhsan Kutlar is an Associate Professor in Mechanical Engineering Department at University of Gaziantep since June 21, 2012. He received his BS/MSc in Mechanical Engineering from the Middle East Technical University Gaziantep Campus at Gaziantep, Turkey and earned his doctoral degree in 1993 in Thermofluids Division of Mechanical Engineering at Liverpool University. He is currently a Senior Lecturer in Mechanical Engineering Department at University of Gaziantep where he teaches classes in thermodynamics, fluid mechanics, hydraulic machinery, mechanical engineering laboratory, computational fluid dynamics and turbulence modelling.

### Prof. Dr. Mehmet Halûk AKSEL

M. Halûk Aksel received his BSc and MSc degrees from the Middle East Technical University, Ankara, Turkey and PhD in Mechanical Engineering from the Lehigh University, Pennsylvania, USA. He is currently a Professor of Mechanical Engineering at the Middle East Technical University, Ankara, Turkey. His research interests include computational fluid dynamics, turbomachinery, turbulence modelling, and gas dynamics. He is the co-author of the book *Gas Dynamics*.